CHAPTER 7

Anticancer potential of Nyctanthes arbor-tristis

7.1 Background

Prostate cancer (PCa) is the most common malignancy in men and second leading cause of cancer in the developed countries. Recent reports from American Cancer Society estimated that around 233,000 new cancer cases and 29,480 deaths tolls from PCa in USA alone in 2014. [334] Though, the incidence and mortality from PCa is lesser in developing countries as compared to other cancer, its incidence and mortality has been on the rising day by day. Several factors are implicated including geographical variation in incidence and prevalence of PCa with life style associated factors are considered as primary concern. [335] The increasing trend estimates that about 1.4 to 1.6 million incidence of PCa and 0.39 to 0.46 million people will die due to PCa in between 2020 and 2025. [2]

The conventional treatment modalities such as chemo-and radio-therapy against PCa are associate with high toxicity and harmful side effects which limits their benefits in prevention of this disease. Also metastatic behavior of PCa and onset of secondary primary tumor (SPT) are additional limitation in conventional treatment. [336] Therefore, newer and alternative approaches are warranted to control the global burden of this disease. Prevention and therapeutic intervention by administration of non-toxic phytochemicals, which targets one or more than one biochemical and molecular pathways involved in carcinogenesis is one of newer approach in this dimension. [17] This preventive and therapeutic approach is found to be effectively reduced cancer burden by preventing the initiational, promotional and progressional phases of carcinogenesis in various experimental models. [152]

Several studies have reported that numerous dietary and non-dietary phytochemicals render strong anticancer efficacy against broad spectrum of cancer including PCa. Among them polyphenolic flavonoids have gained greater attention due to their potential in prevention and intervention of PCa. [337,338] To combat the war against PCa, numbers of phytochemicals such as lycopene, resveratrol, capsaicin, curcumin, silibinin, silymarin etc. have been studied in last few decades. But, none of them is found to be fulfil the desired level of efficacy or fail to cross the clinical trial. [152,153,339]

Therefore, there is a constant demand for new and effective anticancer drugs with no or negligible toxicity. With this background, in the present study, an attempt has been made to examine the anticancer efficacy of free flavonoid fraction of flowers of *Nyctanthes arbor-tristis* Linn. (F^3NAF) and associated molecular mechanism in human PCa PC3 and LNCap cells. The findings of the study demonstrated for the first time that F^3NAF inhibit the growth of PCa cells by inducing G1 and G2 cell cycle arrest along with inhibition of invasive and migratory potentials. Molecular mechanistic aspect of F^3NAF efficacy implicated strong correlation in between cell cycle arrest and decrease in cell cycle regulatory proteins. Furthermore, modulation of signaling pathways (Akt/ERK/mTOR) also contribute to the observed anticancer efficacy of F^3NAF.

7.2 Materials and methods

7.2.1 Chemicals and reagents

Dimethyl sulfoxide (DMSO), 3-(4,5-dimethylthiazol-2-yl)-2,5-diphenyltetrazolium bromide (MTT), propidium iodide (PI), RNAse, Crystal Violet etc. were obtained from Sigma Chemical Co. (St. Louis, MO, USA). RPMI 1640, Fetal bovine serum (FBS), PenStrep, Trypan blue etc. were procured from Gibco, BRL, Maryland, USA. BrdU Cell Proliferation ELISA kit was obtained from Roche diagnostic, Germany. Trans-well chambers, Annexin V-FITC kit was procured from BD Biosciences, San Jose, CA, USA. DCA protein assay kit was obtained from Bio-Rad, Hercules, CA, USA. ECL detection system and anti-mouse peroxidase conjugated secondary antibody were from GE Healthcare (Buckinghamshire, UK). All other reagents were obtained in their commercially available highest purity grade.

7.2.2 Antibodies

Antibody against phospho-Akt (Ser473), phospho-p44/42 MAPK (Erk1/2) (Thr202/Tyr204), p44/42 MAPK (Erk1/2), phospho-EGFR (Tyr1173), phosphor-EGFR (Tyr1068), phospho-mTOR (Ser2448), mTOR, Rictor, MMP9, Akt, VEGF Receptor 2, Cleaved PARP, PARP, Caspase-3 and anti-rabbit peroxidase conjugated secondary antibody were from Cell Signaling Technology (Beverly, MA, USA). Cdk4, Cdk6, cyclin D1, cyclin D3, cyclin E, Cdc25C, Cdc2, Akt1, Nrf2, EGFR, p27, p21 and HRP conjugate β-Actin antibody were from Santa Cruz Biotechnology, Inc. (Santa Cruz, CA, USA). Antibody against MMP2 was obtained from Millipore, USA.

7.2.3 Cell lines and culture

Human non-small cell lung cancer cell lines NCI-H1299 (ATCC® CRL-5803™), A549 (ATCC® CCL-185™); Prostate cancer cell lines PC-3 (ATCC® CRL-1435™), LNCaP (ATCC® CRL-1740™) and human colon cancer cell line SW480 [SW-480] (ATCC® CCL-228™) were obtained from American Type Culture Collection (ATCC), Manassas, VA, USA. All the cell lines except PC-3 were cultured in RPMI 1640 supplemented with 10% fetal bovine serum and 1% penicillin-streptomycin and maintained at 37^0C, 5% CO^2 in incubator. The PC-3 cells were maintained in RPMI 1640 supplemented with 10% heat inactivated fetal bovine serum and 1% penicillin-streptomycin and maintained.

7.2.4 Preparation of fractionated extract

7.2.4.1 Free and bound phenolics rich fraction

The free and bound phenolics was fractionated following the well-established solvent extraction method. [340-342] The powdered forms of plant material was extracted 5 times with 70% ethanol and the supernatant obtained was concentrated. The pH of the concentrated ethanolic extract was adjusted to 1.5 with 4 M HCl and re-extracted with ethyl acetate. The free phenolics fraction containing ethyl acetate extract was filtered through anhydrous sodium sulphate and dried. The dried fraction was re-dissolved in methanol and concentrated and finally dried forms of free phenolics was stored at -20^0C.

The marc obtained after initial ethanolic extraction was re-extracted with 1 M NaOH and the supernatant was collected. The supernatant was acidified with 4 M HCl to pH 1.5 and partitioned into ethyl acetate. The bound flavonoid containing ethyl acetate fraction was dried and finally dried form of fraction was stored at -20^0C.

7.2.4.2 Free and bound flavonoids rich fraction

The free and bound flavonoid rich fraction was extracted following the procedure as described by Subramanian and Nagarajan (1969) and Krishna and Renu (2013) with slight modification. [343,344] The powdered forms of plant material was extracted with 80% methanol for 24 hours using soxhlet apparatus. The methanolic extract was filtered, concentrated, and sequentially extracted by partitioning with petroleum ether (40-60^0C),

ethyl ether and ethyl acetate. Each of the partitioning phase was repeated thrice to ensure complete extraction of phytoconstituents. The ethyl ether fraction containing the free flavonoid and ethyl acetate fraction containing bound flavonoids were concentrated. The dried form of ethyl acetated fraction was stored at -20°C.The ethyl acetate fraction was further acid hydrolyzed for 2 hours by adding 7% H_2SO_4 (10ml/gm residue), filtered and re-extracted with ethyl acetate using separating funnel. The upper ethyl acetate layer containing bound flavonoid was collected from the aqueous layer, washed with distilled water, dried and finally dried form of the extracted fraction was stored at -20°C.

7.2.4.3 Alkaloids rich fraction

The alkaloid rich fraction was extracted by solvent extraction method. [157] The powdered forms of plant material was defatted with petroleum ether and the marc obtained thereafter were moisten and render alkaline with ammonia solution. Then the marc was macerated in diethyl ether in shaking condition for 72 hours and filtered. After twice maceration, the filtrate was concentrated, acidified with dil. H_2SO_4 to pH 3.0-4.0, and the acidified fraction was separated successively three times from the organic fraction by using separating funnel. The alkaloid containing aqueous phase was made alkaline with Na_2CO_3 to pH 9.0-10.0 and partitioned thrice into chloroform and the chloroform was distilled off and finally dried form of fraction was stored at -20^0C.

7.2.5 Screening of fractions

The effective fraction was selected by comparing the IC_{50} values at 24 hours determined from MTT assay. Briefly, the cell lines were seeded at a density of ~1 $X10^3$ cells/well in 96-well plate overnight and subsequently treated with different fractions at concentration ranging from 6.25-200 µg/ml in DMSO for 24-72 hours. At the end of each treatment duration, cells were treated with 10 % MTT dissolved in complete media for 3 hours. Media was discarded and formazan crystals formed were dissolved in DMSO and optical density was measured at 570 and 690. The % cell viability was calculated considering the control of 24 hours as 100 %. The IC_{50} value was calculated from the linear Regression line.

7.2.6 Anticancer activity of F^3NAF against human prostate cancer (PCa) cells

7.2.6.1 Cell growth and viability assay

PC3 and LNCaP cells were seeded at the density of ~5 $X10^4$ cells/well in 6-well plate overnight and subsequently treated with F^3NAF at concentration ranging from 25 to 100 µg/ml in DMSO for 24-72 hours. At the end of each treatment time, cells were collected by brief trypsinization and washed with PBS. Total cell number and dead cell number were determined using a hemocytometer after trypan blue staining. Photomicrographs of treated and control cells were taken using Canon Power Shot A640 digital camera (at 100x magnification) on Zeiss inverted microscope.

7.2.6.2 Cell proliferation assay

The antiprolifeartive efficacy of F^3NAF was evaluated using Colorimetric BrdU Cell Proliferation ELISA kit following manufacturer protocol. Briefly, PC3 and LNCap cells were seeded (~2 $X10^3$ cells/well) overnight in 96-well plates, treated with F^3NAF (12.5 to 100 µg/ml) 24 hours. At the end of incubation period, cells were labeled with 10 µM BrdU and re-incubated for 3 hours. After discarding the labelling solution, FixDenat solution was added and kept for 30 minutes. The FixDenat solution was removed and anti-BrdU-POD solution was added for 90 minutes followed by washing and addition of substrate solution. After 10 minutes stop solution was added and absorbance was measured at 450 nm and 690 nm.

7.2.6.3 Apoptosis assay

Apoptotic cell death analyzed using Annexin V-FITC kit through flow cytometer according to the manufacturer's protocol. The PC3 cells (60–70% confluent) were treated with F^3NAF (12.5, 25 and 50 µg/ml) for 24-48 hours in complete medium. After incubation, both adherent and floating cells were collected by trypsinization, washed twice with ice-cold PBS, and the single cell suspension was stained with 1x Annexin V-FITC binding buffer followed by incubation with Annexin V-FITC and PI in dark for 20 minutes. The fluorescence of the cells was analysed by flow cytometer.

7.2.6.4 Cell cycle analysis

The PC3 cells (60–70% confluent) were treated with F^3NAF (12.5, 25 and 50 µg/ml) for 24 hours in complete medium. After incubation, both adherent and floating cells were collected by trypsinization, washed twice with ice-cold PBS, fixed in ice-cold 70% ethanol for 1hour at -20°C and subsequently incubated with PI (20 µg/ml) and RNase A (200 µg/ml) for another 30 minutes at 37°C. Data acquisition was performed with a fluorescence-activated cell analyzer (FACS Canto, Becton-Dickinson, Franklin Lakes, NJ). For each sample, 10,000 events were acquired and the analysis was carried out using BD FACSDiva software.

7.2.6.5 Clonogenic assay

PC3 cells were plated in 6-well plates at a density of ~0.5 x10^3 cells/well overnight. Next day, cells were treated with DMSO or F^3NAF (12.5, 25 and 50 µg/ml) maintained for 8 days. At the end of treatment, cells were washed twice with ice cold PBS, fixed with a mixture of methanol and glacial acetic acid (3:1) for 10 minutes and then stained with 1% crystal violet in methanol for 15 minutes followed by washing with deionized water. Colonies with more than 50 cells were scored and counted under the microscope. Representative photomicrographs were scanned after staining the cells using HP Scanerjet. [345]

7.2.6.6 Wound healing assay

The anti-migratory efficacy of F^3NAF was examined using the well-established wound healing assay. [345] Briefly, PC3 cells were grown to full confluence in six-well plates and wounded by pipette tips and washed twice with media to remove detached cells. Photomicrographs of initial wounds were taken using Canon Power Shot A640 digital camera (at 100X magnification). Thereafter, cells were treated with DMSO or F^3NAF (12.5, 25 and 50 µg/ml) along with 0.5 µM mitomycin C. Before wounding, cells were made quiescent by pre-treating with 0.5 µM mitomycin C for 2 hours to ensure that wounds are filled due to cell migration and not by cell proliferation. [346] Experiment was terminated as soon as wound was completely filled in DMSO-treated controls (22 hours)

and photomicrographs of final wounds were taken for each group. Initial and final wound sizes were measured using AxioVision Rel.4.7 software, and velocity was calculated using the formula: [{(Initial wound size - final wound size)/2}/22].

7.2.6.7 Transwell invasion and migration assay

The invasion assay was performed using matrigel coated trans-well chambers following established protocol. [347,348] In briefly, the bottom chambers were filled with complete media and top chambers *i.e.* trans-well chambers were seeded with ~2 × 10^4 cells/well in RMPI media containing 0.5% FBS along with DMSO or F^3NAF (12.5, 25 and 50 µg/ml). After 18 hours of incubation under standard culture conditions, non-invasive PC3 cells on top surfaces of the membrane were scraped with cotton swabs and invasive cells on bottom sides of membrane were fixed with cold methanol, stained with hematoxylin/eosin and mounted. Images were taken using Cannon Power Shot A640 camera on Zeiss inverted microscope and invasive cells were manually counted at 400× in 10 random fields on each membrane. Migration assay was performed in similar way to above, but using trans-well chambers without having matrigel layer. [347]

7.2.6.8 Western blotting

After the desired treatment, cell lysate were prepared in non-denaturing buffer. The protein concentration of lysates was estimated using Bio-Rad DC protein assay kit. 40-60 µg of protein samples were subjected to SDS-PAGE on 8-16% tris-glycine gels and blotted onto nitrocellulose membranes followed by blocking with 5% non-fat milk powder (w/v) in Tris-buffered saline (10 mM Tris-HCl, pH 7.5, 100 mM NaCl, 0.1% Tween 20) for 1 hour at room temperature. Membranes were probed with specific primary antibody for 2 hours at room temperature and then overnight at 4°C followed by appropriate peroxidase-conjugated secondary antibody for 1 hour at room temperature and visualized by ECL detection system. Each membrane was stripped and re-probed with peroxidase-conjugated β-actin antibody to ensure equal protein loading. The intensity of bands was determined by scanning the blots with Adobe Photoshop 6.0 (Adobe Systems Inc., San Jose, CA) and the relative intensity as presented below the bands as 'fold change' was calculated by normalizing with β-actin. [345]

7.2.6.9 Statistical analysis

Statistical analysis was performed using SigmaStat 2.03 software (Jandel Scientific, San Rafael, CA). Data were analyzed using one way ANOVA and a statistically significant difference was considered at $p \leq 0.05$, $p \leq 0.01$ and $p \leq 0.001$.

7.2.7 Phytochemical characterization of F^3NAF by HR LCMS analysis

The high resolution liquid chromatography mass spectrometry (HR LCMS) was carried out in positive ion mode using Chipcube, 6550 iFunnel Q-TOF B.05.01 (B5125.1) (Agilent Technologies, USA) mass spectrometer equipped with electrospray ionization source. UPLC was performed using 1290 Infinity UHPLC System, 1260 infinity Nano HPLC [using a ZORBAX C18 (2.1 x 50mm, 1.8 μm) column (Agilent Technologies, USA)]. The mobile phase consisting of water and acetonitrile (CH_3CN) was used at a flow rate 0.3 ml/minute. The gradient of mobile phase started with 95:5 (CH_3CN:H_2O) for 20 minutes and then changed to 5:95 (CH_3CN:H_2O) for 10 minutes and finally returned to 95:5 (CH_3CN:H_2O). The spectra was acquired using UHPLC PDA Detector in the mass range from 60 to 1000 (m/z) at the rate of 1 spectra/second. The analysis was carried out at Sophisticated Analytical Instrument Facility (SAIF), Indian Institute of Technology, Bombay (IIT, Bombay).

7.3 Results

7.3.1 Selection of active fraction

The most active fraction was selected from the pool of ten (10 Nos.) fractions against five (05 Nos.) human cancer cell lines by measuring the IC_{50} values at 24 hours. Out of the 10 fractionated extract the free flavonoid rich fraction of *Nyctanthes arbor-tristis* (F^3NAF) was found to be more promising against lung cancer (H1299 and A549) and prostate cancer (PC3 and LNCap) cell lines. The selection of cell lines in this study is based on their availability in our laboratory. [Annexure VII]

Table 44: Effects of fractionated extract on viability of lung, prostate and colon cancer cell line

Fractions	Cells ->	Lung cancer		Prostate cancer		Colon cancer
	Code	H1299	A549	PC3	LNCap	SW480
Fraction 1	FPFNAF	---	+	++	---	---
Fraction 2	F^3NAF	+++	++	+++	+++	---
Fraction 3	BF^2NAF	---	---	---	+	---
Fraction 4	AFNAF	+	+	++	---	++
Fraction 5	SFNAF	+	---	---	---	---
Fraction 6	FPFPTL	---	---	++	---	---
Fraction 7	BPFPTL	---	---	++	---	---
Fraction 8	F^3PTL	---	---	+	---	---
Fraction 9	BF^2PTL	---	---	---	---	---
Fraction 10	AFPTL	++	++	+	---	+

Table 40: Screening of active fractions against human cancer cell line. IC_{50} values are calculated as average of 24 hours. Upto 250µg/ml : +++ ; 251-500 µg/ml : ++ ; 501-1000 µg/ml : + ; Above 1000 µg/ml : ---.

Abbreviations:

FPNAF: Free Phenolic fraction of *Nyctanthes arbor-tristis* flower

F^3NAF: Free flavonoid fraction of *Nyctanthes arbor-tristis* flower

BF^2NAF: Bound flavonoid fraction of *Nyctanthes arbor-tristis* flower

AFNAF: Alkaloid fraction of *Nyctanthes arbor-tristis* flower

SFNAF: Saponin fraction of *Nyctanthes arbor-tristis* flower

FPFPTL: Free Phenolic fraction of *Phlogacanthus thyrsiflorus* leaf

BPFPTL: Bound Phenolic fraction of *Phlogacanthus thyrsiflorus* leaf

F^3PTL: Free flavonoid fraction of *Phlogacanthus thyrsiflorus* leaf

BF^2PTL: Bound flavonoid fraction of *Phlogacanthus thyrsiflorus* leaf

AFPTL: Alkaloid fraction of *Phlogacanthus thyrsiflorus* leaf

7.3.2 F^3NAF exhibit anticancer activity against human prostate cancer cells

7.3.2.1 F^3NAF inhibit of growth of PCa cells

To determine the effect of F^3NAF on PCA cells, in the first experiment PC3 and LNCaP cells were treated with various doses of F^3NAF (25-100 µg/ml), and its effect on total cell number and cell death were analyzed as a function of time (24, 48 and 72 hours) by Trypan blue exclusion assay. As shown in Figure 35(A) and 36(A), F^3NAF showed

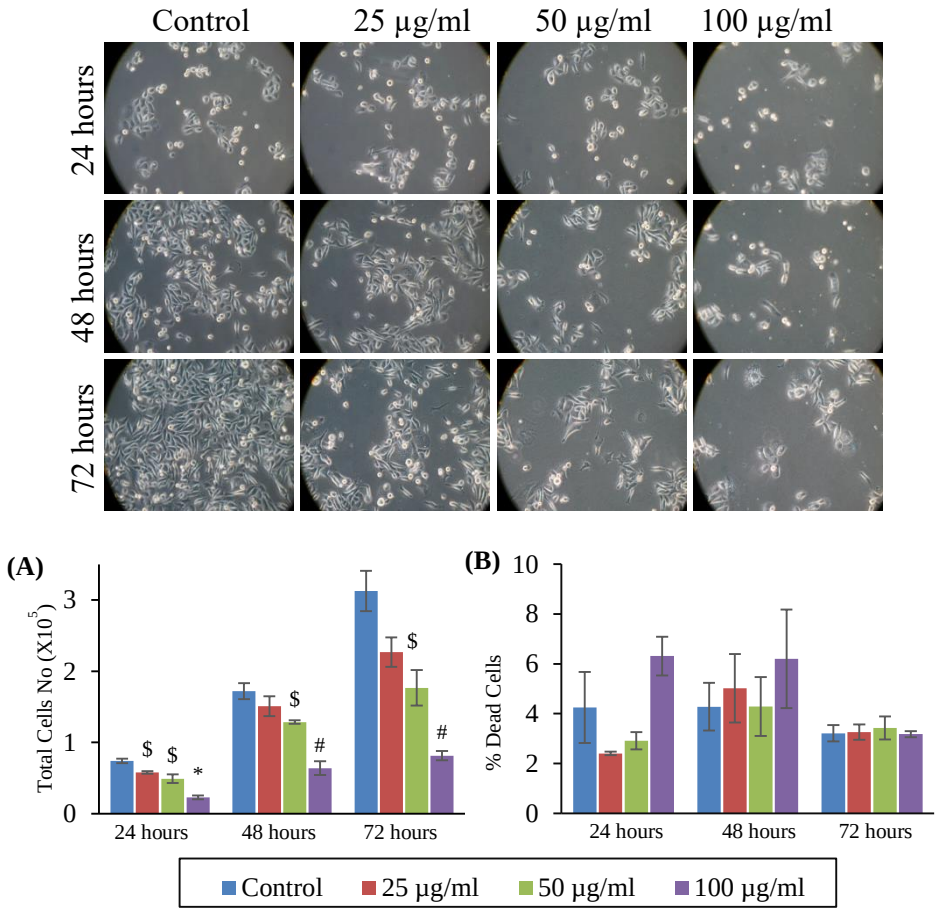

Figure 35: F^3NAF inhibit the growth of PC3 cells: PC3 cells were treated with DMSO or F^3NAF (25-100 µg/ml) in complete media for 24-72 hours. At the end of each treatment time, cells were harvested and counted as mentioned in 'Material and Methods', and (A) total cell number and (B) % dead cells are shown. The values are represented as mean ± SEM of three samples for each treatment. $, $P < 0.05$; #, $P < 0.01$; *, $P < 0.001$.

inhibition of cell growth in a dose-and time-dependent manner in both PC3 and LNCaP calls. However, the total cell numbers at 48 and 72 hours in both treated and non-treated is greater than the 24 hours. Using the trypan blue dye exclusion method, we observed that the decrease in total cell number is accompanied by an increase in cell death [Figure 35(B) and 36(B)]. The increase in cell death is more prominent, and dose and time dependent in LNCap cells. However, in both the cells, cell death did not increase beyond 12%, suggesting that the overall decrease in total cell number is not due to cell death inducing effects of F^3NAF.

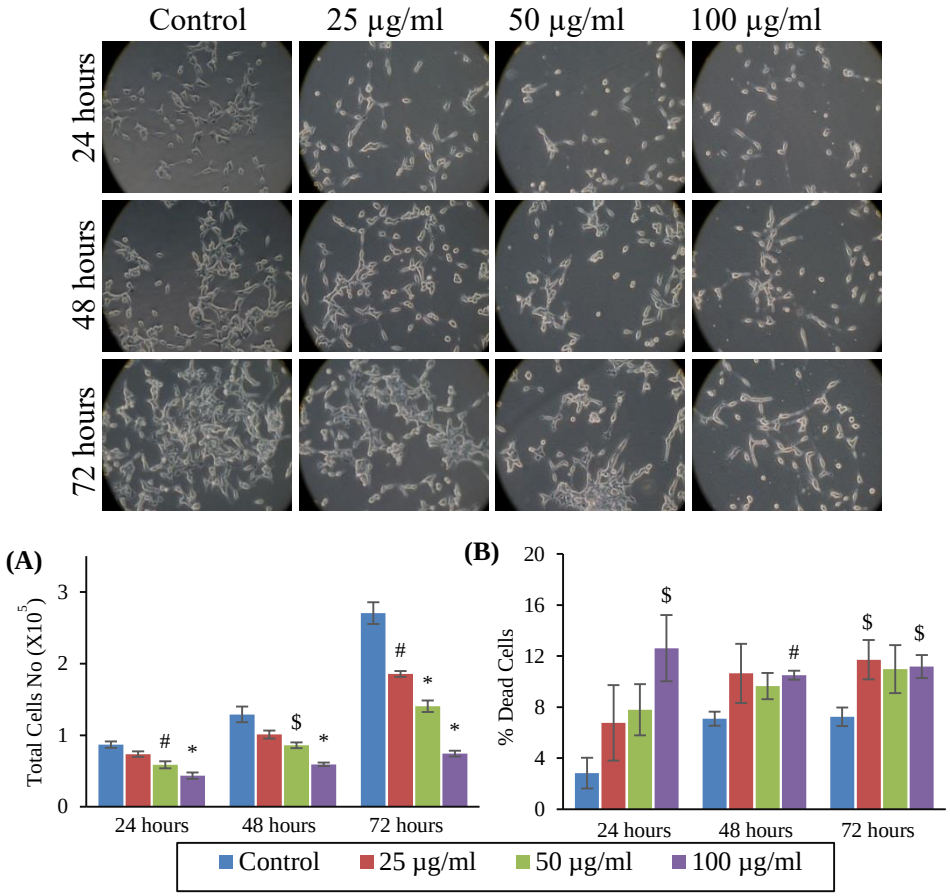

Figure 36: F^3NAF inhibit the growth and caused death of LNCaP cells: LNCaP cells were treated with DMSO or F^3NAF (25-100 µg/ml) in complete media for 24-72 hours. At the end of each treatment time, cells were harvested and counted as mentioned in 'Material and Methods', and (A) total cell number and (B) % dead cells are shown. The values are represented as mean ± SEM of three samples for each treatment. $, $P < 0.05$; #, $P < 0.01$; *, $P < 0.001$.

7.3.2.2 F^3NAF inhibit the proliferation of PCa cells

In order to rule out the inhibition of total cell number, we performed metabolic and replication based assay. The results of MTT assay showed that F^3NAF (6.25-200 µg/ml) decreases the viability of PC3 cells by 0.4-19.2% ($p \leq 0.05–0.01$) and 16.5-88.5% ($p \leq 0.05–0.001$) after 24 and 48 hours of treatment respectively [Figure 37(A)]; and of LNCaP cells by 0.2-27.8% ($p \leq 0.05–0.001$) and 3.1-36.3% ($p \leq 0.05–0.001$) after 24 and

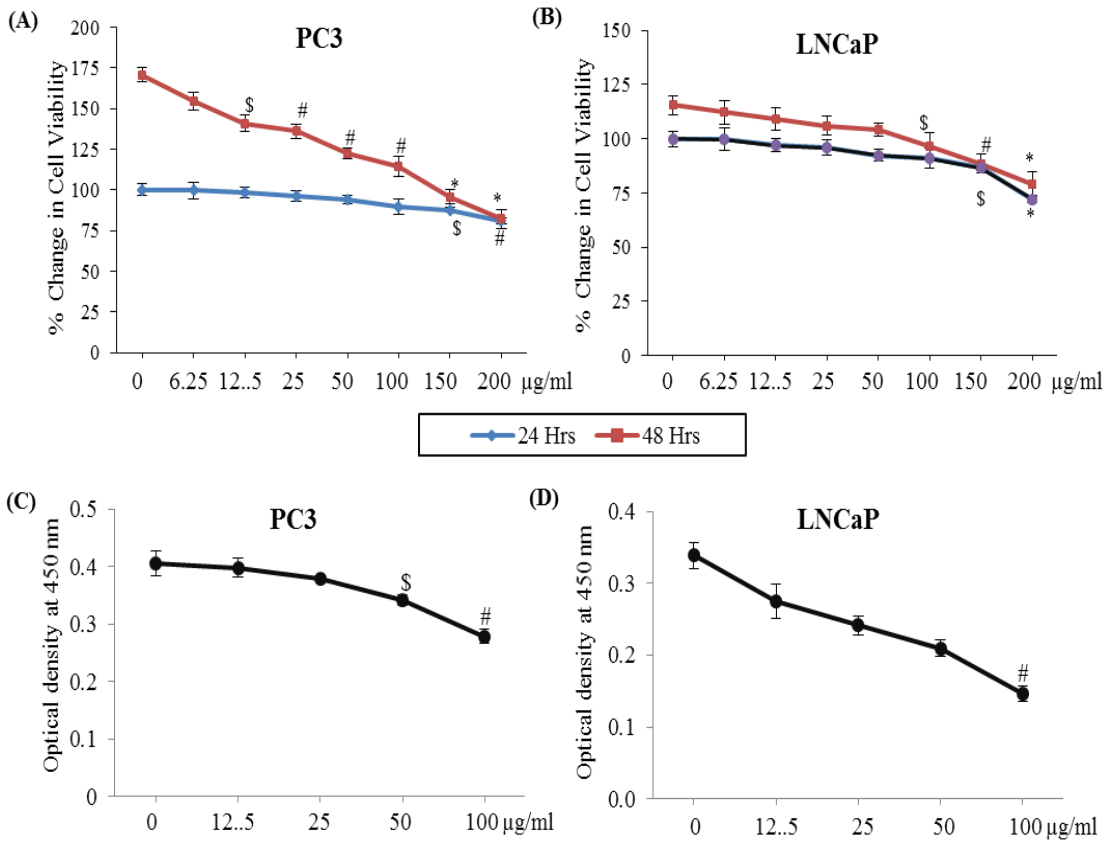

Figure 37: F^3NAF inhibit the proliferation of PC3 and LNCaP cells: PC3 and LNCaP cells treated with various concentration of F^3NAF in DMSO for 24-48 hours. At the end of each treatment duration, proliferation was measured by MTT and BrdU assay as mentioned in 'Material and Methods', and (A-B) % cell viability (MTT assay) and (C-D) optical density at 450 nm (BrdU assay) are shown. The values are represented as mean ± SEM of six (MTT)/four (BrdU) samples for each treatment. $, $P < 0.05$; #, $P < 0.01$; *, $P < 0.001$.

48 hours of treatment respectively [Figure 37(B)]. The replication based BrdU assay, demonstrated inhibition of proliferation upto 31.3% ($p \leq 0.05–0.01$) and 56.7% ($p \leq 0.01$) in PC3 and LNCaP cells, respectively upon F^3NAF (12.5-100 μg/ml) treatment for 24 hours [Figure 37(C,D)]. These results clearly showed that F^3NAF inhibit the proliferation of PCa cells. Therefore, next we examined the effect of F^3NAF on cell cycle progression to determine whether the inhibitory effect on cell proliferation is accompanied by modulation of cell cycle progression.

7.3.2.3 Effect of F^3NAF on apoptosis in PC3 cells

As there was evidence of slight cell death in prostate cancer cells, we examined the effects F^3NAF on induction of apoptosis in PC3 cells by Annexine V-PI staining. As shown in Figure 38, F^3NAF didn't induces apoptotic death in both the time point. To confirm the flow analysis expression level of markers of apoptosis were evaluated by western blot analysis. F^3NAF treatment didn't cause change in the levels of cleaved PARP and caspase 3, confirmed our observation.

7.3.2.4 F^3NAF arrest progression of cell cycle at G1 and G2 phase in PC3 cells

To determine the cause of anti-proliferative potentials of F^3NAF, we examined the progression of cell cycle of PC3 cells by flow cytometer. Cell cycle distribution analysis showed that F^3NAF treatment results in a dose dependent increase in G1-phase cells at all the treated doses and decrease of cells in subsequent phases. The decrease in the G2 phase is observed to be dose dependent and was found to be significant. The cells in S-phase and G0-phase were differentially modulated on F^3NAF treatment. At the highest dose of F^3NAF, the G0-phase cells is increased, suggesting that F^3NAF favours the cells to enter resting phase, rather than entering into cell division. These data clearly suggest that the inhibition of proliferation is accompanied by G1 and G2 phase cell cycle arrest [Figure 39]. Further, we analyzed the molecular basis of these halting of cell cycle phase at G1 and G2.

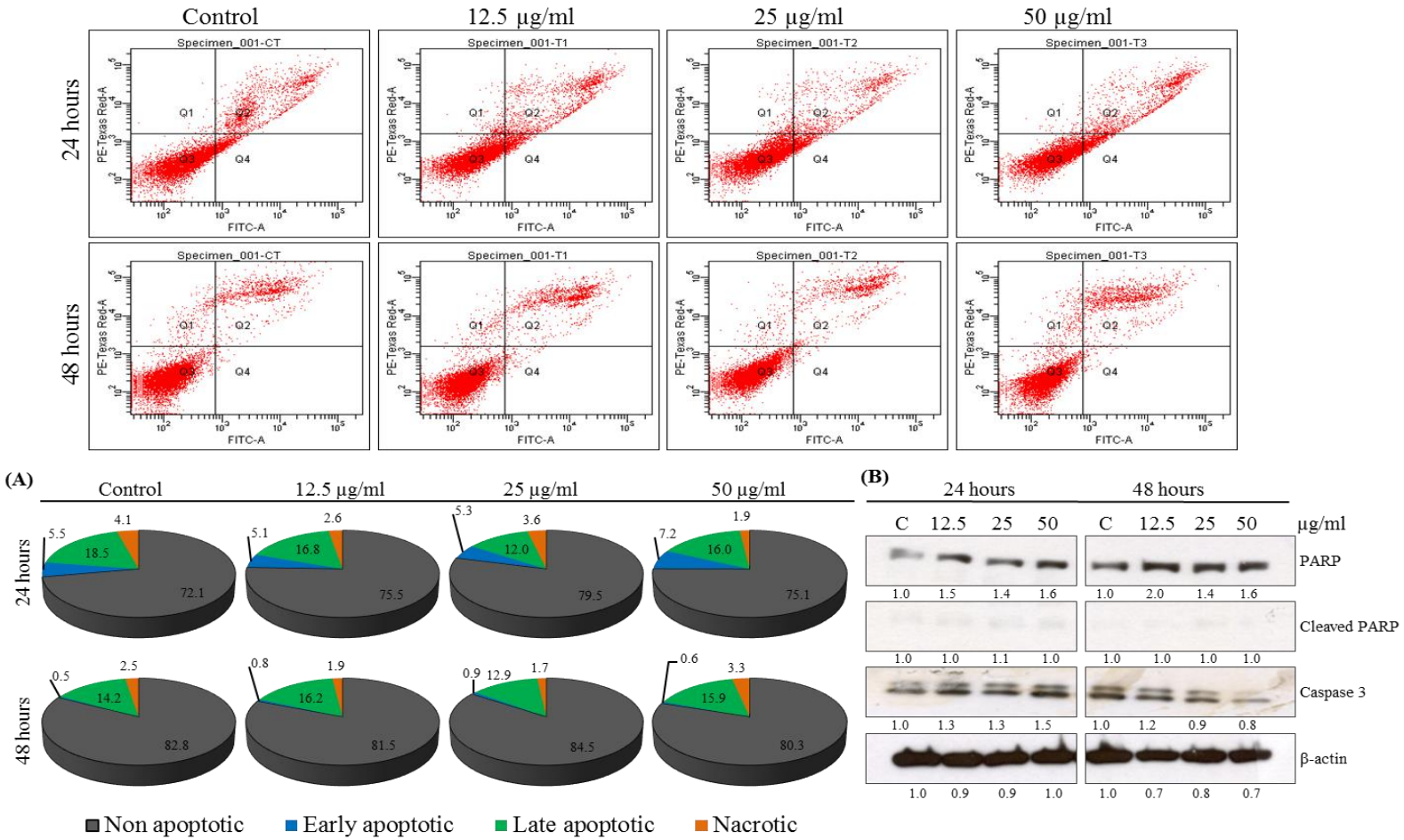

Figure 38: Effects of F^{3}NAF on apoptosis in PC3 cells: The PC3 cells were treated with various concentration of F^{3}NAF in DMSO for 24 hrs. At the end of treatment duration, apoptosis were studied using Flow cytometer by Annexine V/PI staining. The expression level of markars of apoptosis were examined by western immunoblotting techniques. The values represent the relative intensity of each band which is normalized by the respective β-actin. C: Control.

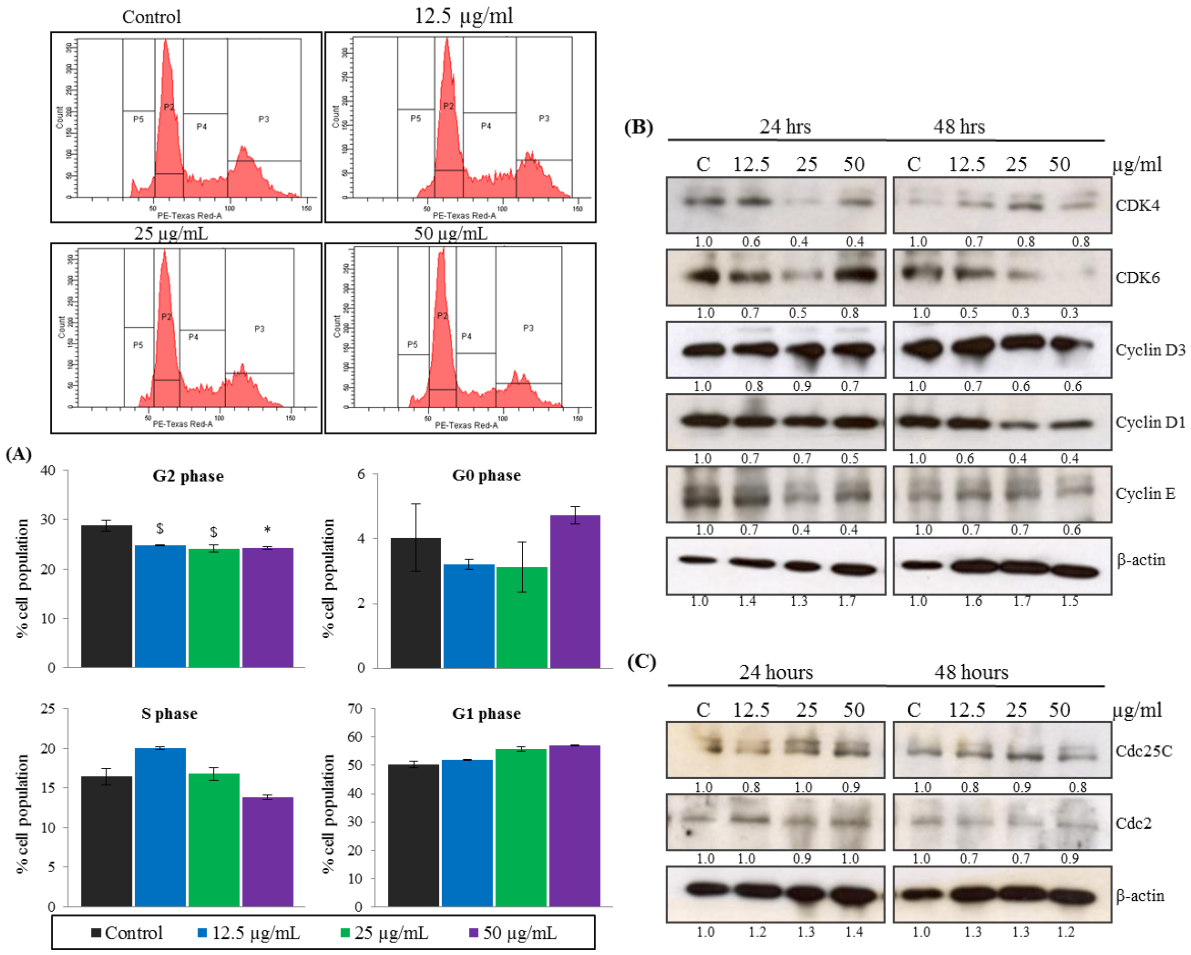

Figure 39: F[3]NAF cause arrest in progression of cell cycle of PC3 cells and modulates regulators of cell cycle: The PC3 cells were treated with various concentration of F[3]NAF in DMSO for 24 hours. At the end of treatment duration, distribution of cell cycle was determined using Flow cytometer as mentioned in 'Material and Methods', and (A) % of cell populations were shown. The expression level of regulators of cell cycle were examined by western immunoblotting techniques as mentioned in 'Material and Methods', and (B) G1 phase cell cycle regulators and (C) G1 phase cell cycle regulators were shown. The values represent the relative intensity of each band which is normalized by the respective β-actin. C: Control.

7.3.2.5 F[3]NAF modulate the regulators of G1 and G2 phase of cell cycle in PC3 cells

Since, progression of cell cycle is mediated by CDKs in complex with corresponding cyclins, we analyzed the level of CDKs and cyclins involved in G1 phase of cell cycle in PC3 cells. Western blot analysis revealed that F[3]NAF treatment for 24 and 48 hours

results in remarkable decrease in expression level of CDK4, CDK6, cyclin D1, cyclin D3 and cyclin E [Figure 39(A)]. As, F^3NAF treatment also resulted in G2 arrest in PC3 cells, we also examined the expression level of regulators of G2 phase of cell cycle. The level of Cdc25C and Cdc2 were observed to be decrease upon treatment with F^3NAF; however, the decrease was very prominent after 48 hours of treatment [Figure 39(B)].

7.3.2.6 F^3NAF inhibits the clonogenicity of PC3 cells

To confirm the above findings of anti-proliferative potentials of F^3NAF, we determined the effect of F^3NAF treatment on the colony forming potential of PC3 cells in the clonogenic assay. As shown in Figure 40, F^3NAF treatment (12.5, 25 and 50 µg/ml) inhibited the clone formation by PC3 cells in dose dependent manner by 17.6-54.3% ($p \leq 0.05$-0.001) and highest dose i.e. 50 µg/ml inhibited upto 54.3% as compared to control [Figure 40].

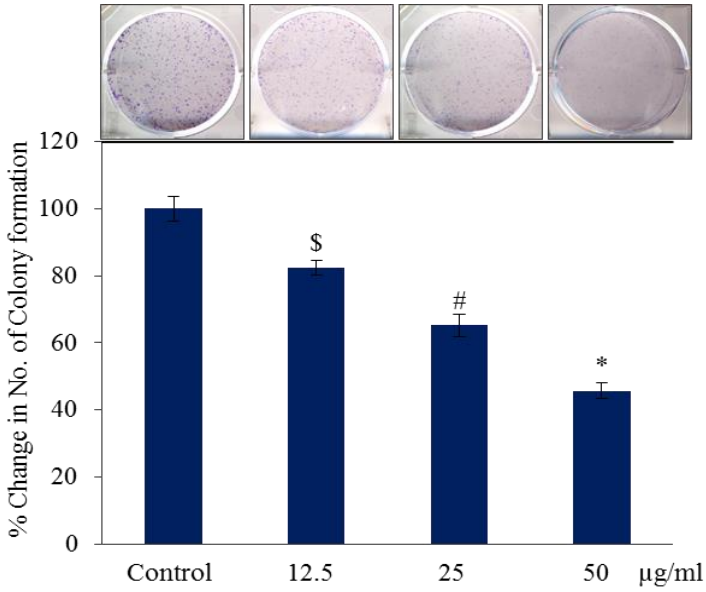

Figure 40: F^3NAF inhibit the clonogenicity of PC3 cells:he PC3 cells were treated with various concentration of F^3NAF in DMSO for 8 days. At the end of treatment duration, cells stained with 0.1 % Crystal violet and counted as mentioned in 'Material and Methods', and % change in number of colony formation was shown. Representative photomicrographs were scanned after staining the cells using HP Scanerjet. The data shown are mean ± standard error of mean of three samples for each treatment. $, $P < 0.05$; #, $P < 0.01$; *, $P < 0.001$.

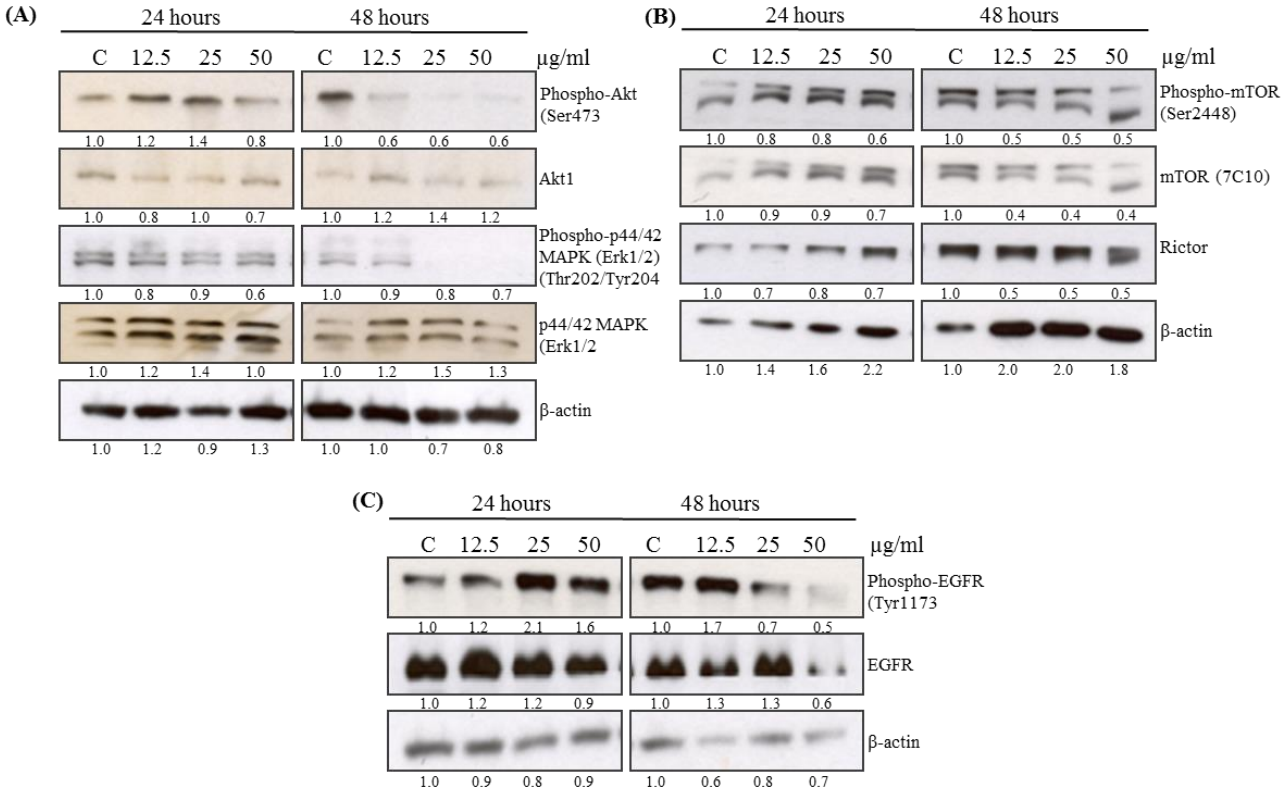

Figure 41: F^{3}NAF modulate the regulators of growth, proliferation and survival in PC3 cells: The PC3 cells were treated with various concentration of F^{3}NAF in DMSO for 24-48 hours. At the end of treatment duration, cell lysate were prepared and expression level were examined by western immunoblotting techniques as mentioned in 'Material and Methods'. The values represent the relative intensity of each band which is normalized by the respective β-actin. C: Control.

7.3.2.7 F^{3}NAF modulate the regulators of growth, proliferation and survival in PC3 cells

To understand the signaling pathways targeted by F^{3}NAF, we analyzed the expression levels of few signaling molecules. Western blot analysis revealed that F^{3}NAF treatment for 24 and 48 hours results in remarkable changes in the expression level of signaling molecules. The phosphorylation of Akt at Ser 473, EGFR at Tyr1173 increased initially and thereafter decreased prominently. In contrast to Akt and EGFR, phosphorylation of

p44/42 MAPK(Erk1/2) at Thr202/Tyr204, and mTOR at Ser2448 were found to be remarkably decreased in both the time points. There were also evidence of significant decrease in the expression level of Rictor mTOR [Figure 41].

7.3.2.8 F^3NAF exerts strong anti-migratory and anti-invasive efficacy against PC3 cells

F^3NAF treatment (12.5-50 µg/ml) inhibited the wound closer potential of PC3 cells by 8.2-73.7% ($p \leq 0.05–0.001$), in a dose-dependent manner [Figure 42(C)]. In this assay, the migration of PC3 cell was only due to cellular mobility as they were treated with mitomycin C. The migratory potential of PC3 cells was also examined using trans-well chambers. In this assay, F^3NAF treatment (12.5-50 µg/ml) inhibited migratory potential of PC3 cells by 4.4-34.6% ($p \leq 0.05–0.01$), in a dose-dependent manner [Figure 42(A)]. Next, we examined effects of F^3NAF on the invasive potential of PC3 in well-established invasion assay using matrigel coated trans-well chambers. In this assay, the cells need to invade the matrigel which mimics the extra-cellular matrix, the first barrier during cancer cells invasion. Results showed that F^3NAF inhibits invasive potential of PC3 ells by 13.7-59.9% ($p \leq 0.05–0.001$), in a dose-dependent manner [Figure 42(B)]. Since, the investigated doses of F^3NAF don't exert toxic effect at around 24 hours, as deduce from cell death data, the anti-migratory and anti-invasive efficacy is remarkable.

7.3.3 Chemical characterization of F^3NAF

To characterize the phytochemical present in the F^3NAF, the sample was subjected to HR LCMS analysis. The total ion chromatogram (TIC) of HR LCMS highlighted the presence of large group of compounds [Figure 43]. The individual components present in F^3NAF were identified by comparing their MS/MS spectra with database. The HR LCMS indicated the presence of flavonoids such as Epigallocatechin gallate, Phloridzin, Quercetin etc. It also contain Methyl jasmonate, Ginkgolide A, B, Isovaleric acid, Mitoxantrone, Deutzioside, Citronellic acid. The phytochemicals present in the major peak is shown in the figure. [Annexure VIII]

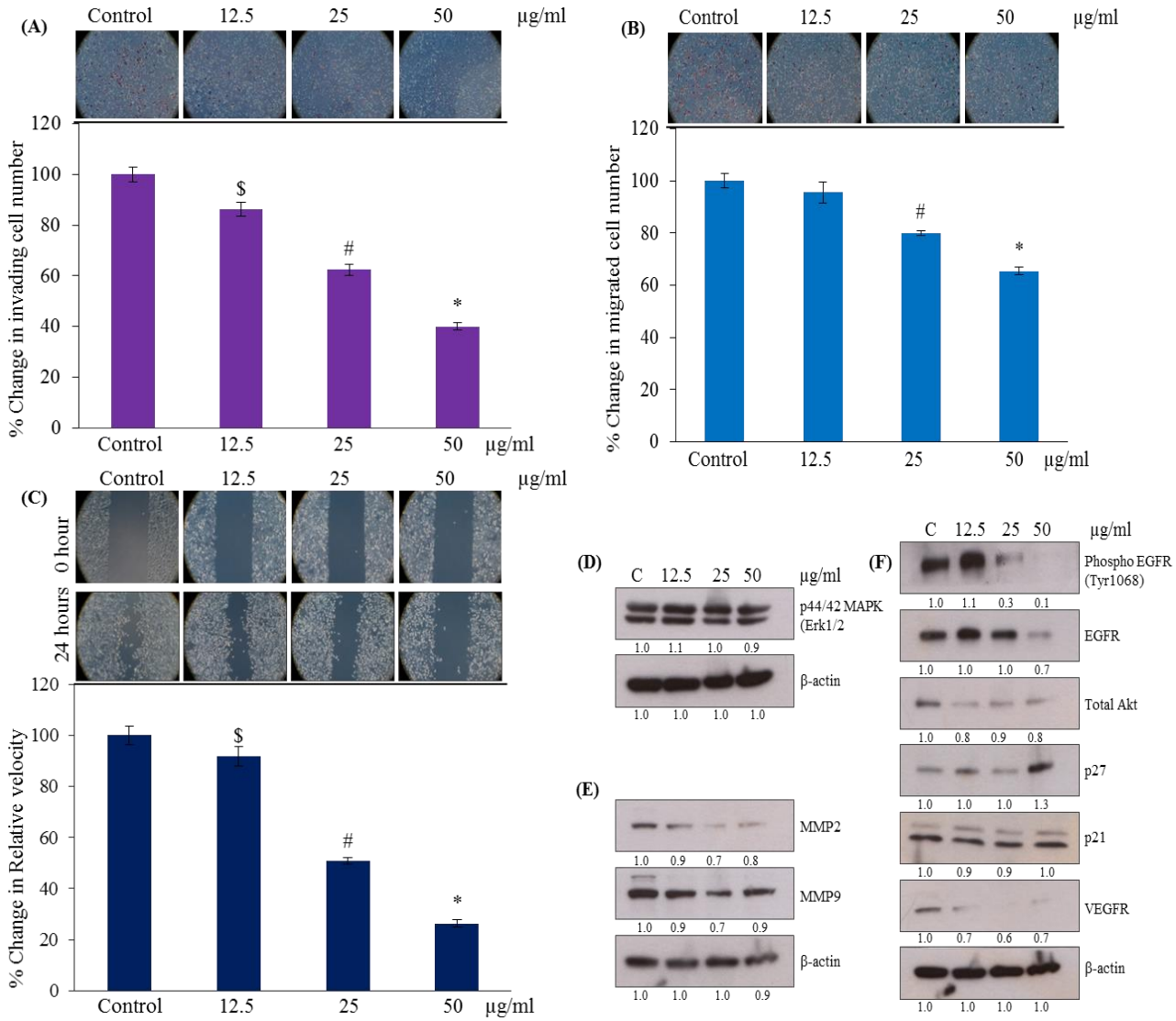

Figure 42. F^{3}NAF inhibit the migration and invasion of PC3 cells: The PC3 cells were treated with various concentration of F^{3}NAF and anti-migration and anti-invasion assay were performed as mentioned in 'Material and Methods', and (A) % change in invading cells, (B) % change in migrated cells number and (C) % change in relative velocity were shown. The expression level of molecules involved in migration and invasion were examined by western immunoblotting techniques as mentioned in 'Material and Methods'. The data shown are mean ± standard error of mean of three samples for each treatment. $, $P < 0.05$; #, $P < 0.01$; *, $P < 0.001$.

A)

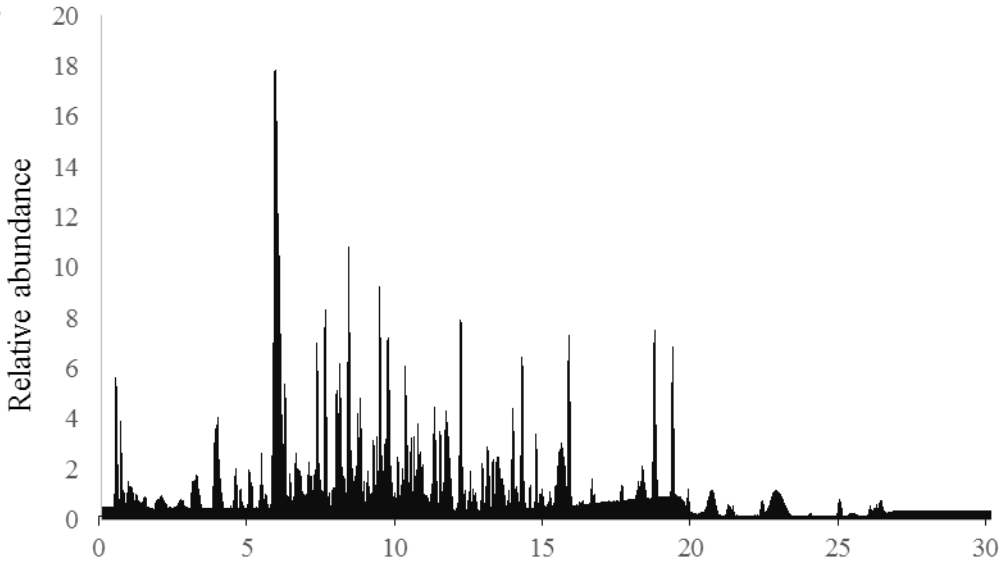

B)

Sl. No.	RT	Mass	Name	Formula
1	5.799	196.1094	Benzenemethanol, 2-(2-aminopropoxy)-3-methyl-	$C_{11}H_{16}O_3$
2	5.878	102.0676	Isovaleric acid	$C_5H_{10}O_2$
3	5.878	168.1145	2E,7E-decadienoic acid	$C_{10}H_{16}O_2$
4	5.878	126.104	4-octenal	$C_8H_{14}O$
5	5.878	140.1196	2-nonenal	$C_9H_{16}O$
6	5.879	156.1144	beta-nonylenic acid	$C_9H_{16}O_2$
7	5.893	186.125	9-hydroxy-2E-decenoic acid	$C_{10}H_{18}O_3$
8	6.016	222.1251	Hydroxyibuprofen	$C_{13}H_{18}O_3$

Figure 43: Chemical characterization of F^3NAF: The F^3NAF was analysed by HR LCMS technique as described in material and methods. A) The total ion chromatogram of the F^3NAF and **(B)** phytochemical present in the major peak.

7.4 Discussion and conclusion

The present study examined the anticancer activity of free flavonoid fractions extracted from the flower of *Nycthanthes arbor-tristis* and established strong antiprolifeartive activity against human prostate cancer (PCa). *Nycthanthes arbor-tristis* is a traditional medicinal plant used to treat various forms of ailments and recent pharmacological studies also suggests its antibacterial and cytotoxic, immune-stimulatory,

anti-inflammatory, analgesic, anti-malarial, anti-larvicidal, anti-antioxidative, radical scavenging activities in various preclinical model. [190-198] In our previous study, we have showed that the hydroalcoholic flower extract of this plant inhibited the papilloma incidence and multiplicity as well as papilloma yield and burden against DMBA induced and croton oil promoted skin and B(a)P induced forestomach papillomagenesis. Our biochemical mechanistic study indicated differential modulation of enzymes involved in xenobiotic metabolism and antioxidants and reactive species played role in chemoprevention. Therefore, it is rational and justified to isolate the active fraction/molecule with anticancer activity from this plant.

The idea of evaluating free flavonoid fraction of *Nycthanthes arbor-tristis* for their anticancer potential is based on the presence of high amount of phenolic and flavonoid compound as evident from our earlier study. In the present study, we have analyzed the phytochemical component in the F^3NAF by HR LCMS technique. The analysis clearly indicated that the F^3NAF is rich in flavonoid such as Epigallocatechin gallate, Phloridzin, Quercetin etc. The Epigallocatechin gallate and Quercetin are two well known flavonoids that exhibit antioxidative and anticancer activity in various experimental models. [56,349] The phloridzin is known to possess hepatoprotective, antioxidative activity and exert anticancer activity by inducing apoptosis in human liver cancer cells. [137, 350-352] Beside flvaonoids, Ginkgolide A, B, hexadecanoic acid, isovaleric acid etc. were also detected. This rational strongly our approach to study the anticancer activity of F^3NAF against human prostate cancer (PCa).

Cancer is characterized by excessive and uncontrolled proliferation of cell of any parts of the body of animal system. As such targeting proliferative ability of cell has been widely accepted as therapeutic approach. [353] In this study free flavonoid F^3NAF exhibited strong antiprolifeartive potentials against human prostate cancer cell line (PC3 and LNCap). The F^3NAF inhibited the proliferation of PC3 cells by arresting at G1 and G2 phase of cell cycle. The progression of cell cycle through various phases are regulated by CDKs by forming complexes with cyclins. The transition from G1 to S phase is largely controlled by Cyclin Dependent Kinase 4 and 6 (CDK4 and CDK6) and Cyclin E dependent kinase (CDK2). During early G1 phase of cell cycle, CDK 4 and

CDK6 activates the progression by forming a complex with cyclin D1, D2 and D3. The cyclin-CDK complex phosphorylate Rb protein which in turn release the binding partner E2F. The transcription factor E2F induces expression of several proteins that are required during S phase. [354-356] In the present study, F^3NAF treatment to human prostate cancer cell PC3 resulted in marked down regulation of cyclin D1, D3, E CDK4 and CDK6. Similar kinds of mechanism of antiproliferative activity were reported in case of LNCap cells treated with Vitamin D and PC3 with silibinin and silymarin. The inhibition of these molecular parameters of G1 to S phase transition could have played role in inhibition of proliferation in PC3 Cells. The progression of cell cycle from G2 to M is basically regulated by the activation and deactivation of CDK-regulatory protein and cyclin complexes. Cyclin dependent kinase 2 (CDK2), also known as Cdc2 forms complex with cyclin A and B which drive the progression from G2 to S phase. Increased Cdc2 kinase activity is found in many types of human cancer which allows progression of cell cycle from G2 to M with having defected DNA. The enzymes Cdc25C regulates the progression of cell cycle by phosphorylating CDKs during both G1 to S and G2 to M. [357-360] Therefore, inhibition of Cdc2 is a promising approach to halt the progression of cell cycle. We observed similar inhibition of cdc2 expression and might led to affect cell cycle progression with down regulation of G1 to S phase transition.

Several molecular signaling pathways are implicated in the development and progression of PCa and disruption of such signaling network is being actively pursued as a therapeutic target. The level of membrane bound epidermal growth factor receptor (EGFR) and its autophosphorylated (Tyr1173) form is known to highly express in hormone refractory PCa cell PC3 and DU145, than in LNCap cells, supporting their probable role in malignant transformation into aggressive and metastatic high grade. [361,362] The EGFR upon activated by cognate ligand epidermal growth factor (EGF) activates RAF kinase, a Mitogen-activated protein kinases-kinase-kinase (MAP3K) and finally phosphorylates and activates the effector component though MAPK/ERK MEK kinase-kinase (MAP2K). [363] The activated ERK1/2 further phosphorylate several cytoplasmic and nuclear substrate such as c-Jun, c-Fos, and p53 and ultimately stimulate global protein synthesis and *de novo* nucleotide biosynthesis. The activated ERK1/2 also

promotes transition of cell cycle from G1 to S phase by enhancing accumulation of Cyclin D1, assembling and stabilizing cyclin D1–Cdk4/6 complexes. [364] The downregulation in the level of phosphorylated ERK1/2 (Thr202/Tyr204) by F^3NAF treatment in the present study possibly cause arrest in cell cycle and thereby inhibited proliferation.

The Phosphoinositide 3-kinase/Akt (PI3K/Akt) pathway is one of the central signal transduction pathway which links the functions of many membrane receptor with cellular functions. Akt is activated upon phospholipid binding and subsequent phosphorylation at Ser473 by mTOR in a rapamycin-insensitive complex with rictor and Sin1. The activated Akt in turn activated several downstream targets such as rapamycin-sensitive complex of mTOR with raptor, glycogen synthase kinase 3. Phosphorylated mTOR (Ser 2448) regulates large numbers of cellular process such as cell survival, proliferation, and differentiation etc. In 30-50% of PCa cases, the PI3K/AKT/mTOR signaling is found to be up-regulated. The mTOR signaling is also enhanced by activated ERK1/2 through direct phosphorylation of tuberous sclerosis complex 2 (TSC2) at Ser 664 or via serine/threonine kinase RSK1 at Ser 1798. [365,366] Thus the cooperative role of EGFR, ERK1/2, AKT activate mTOR and promote cell growth. In the present study, F^3NAF inhibited the expression level of mTOR and phosphor-mTOR (Ser 2448) along with rictor protein suggesting that the growth and survival of PC3 is inhibited upstream to Akt phosphorylation or downstream to mTOR. However, the decreased level of Akt phosphorylation after 48 hours of F^3NAF treatment also inhibited the growth and survival.

The major limitation of treatment of cancer with current chemotherapeutic drug is metastatic behaviors of cancer. As the cancer become aggressive it starts to migrate to a distant organ forming secondary tumor over there. In the process of metastasis cancer cells invade the surrounding blood vessel by degrading ECM and migrates. It has been well established that over expression of MMPs facilitates invasion through degradation of ECM. In particular, MMP2 and MMP9 are the two key type IV Collagenase and Gelateinase that degrades the basement membrane of type IV collagen, gelatin and fibronectin during tumor invasion and metastasis. [367,368] Therefore, we have also studied

the inhibitory potential of F^3NAF by wound healing assay and transwell invasion and migration assay using PC3 cells. The results indicates that F^3NAF strongly inhibits the progression of human prostate cancer cells through down regulation of MMP2 and MMP9.

From the findings of this study it can be concluded that free flavonoid fraction of flower of *Nyctanthes arbor-tristis* (F^3NAF) inhibit the proliferation of human prostate cancer cells by arresting cell cycle at G1 and G2 phase through involvement of cell cycle regulatory molecule. Additionally, F^3NAF inhibit the invasion and migration of human prostate cancer PC3 cells by down regulating MMPs. The exciting finding of this study, merits further identification, isolation and investigation of active molecules present in flower of *Nyctanthes arbor-tristis* for their anticancer efficacy and also to elucidate the precise molecular mechanisms.